

Resonance Characteristics Analysis of Grid-connected Inverter Systems based on Sensitivity Theory

Jian Wu[†], Wanqin Han^{*}, Tao Chen^{*}, Jiaqi Zhao^{*}, Binbin Li^{*}, and Dianguo Xu^{*}

^{†,*}School of Electrical Engineering and Automation, Harbin Institute of Technology, Harbin, China

Abstract

Harmonic resonance exists in grid-connected inverter systems. In order to determine the network components that contribute to harmonic resonance and the composition of the resonant circuit, sensitivity theory is applied to the resonance characteristic analysis. Based on the modal analysis, the theory of sensitivity is applied to derive a formula for determining the sensitivities of each network component parameter under a resonance circumstance that reflects the participation of the network component. The solving formula is derived for both parallel harmonic resonance and series harmonic resonance. This formula is adopted to a 4-node grid-connected test system. The analysis results reveal that for a certain frequency, the participation of parallel resonance and series resonance are not the same. Finally, experimental results demonstrate that the solving formula for sensitivity is feasible for grid-connected systems.

Key words: Grid-connected system, Resonance sensitivity, Sensitivity analysis, Series harmonic resonance

I. INTRODUCTION

Nowadays, with the development of distributed energy power generation and micro-grid technologies, a large number of grid-connected converters have been adopted, leading to more and more non-linear loads being connected to distribution networks. Since the impedance characteristics of the converter and the nonlinear load both vary with respect to the frequency, the characteristics of the system are difficult to determine. The resonance characteristics of the distribution network become complex and the analysis of the resonance becomes more difficult.

In the analysis of the resonant characteristics of a grid-connected inverter system, the influence of the inverter impedance characteristics is usually the focus. A single-phase LCL inverter with a double-closed-loop control system, a grid-connected current feedback and a filter capacitor current feedback is described as an impedance model in [1]. In [2], a three-phase grid-connected inverter is modeled in the dq

rotating coordinate system considering the delay time of the digital control. However, the model is complicated and computationally expensive. In [3], a small-signal analysis method is used to model a flyback micro-inverter parallel system, and a Norton equivalent model of the system is obtained. The analysis results show that the resonant point is within a certain frequency range.

At present, frequency spectrum analysis is the most widely used resonance analysis method in electrical systems that can obtain the resonant frequency response by injecting a series of harmonic voltages into each loop or by injecting harmonic currents into each node of the simulation circuit [4]-[6]. However, this method is cumbersome and error-prone, particularly when the electrical system has a complex multi-loop structure. In addition, the relationships between the elements and the elements that result in resonance cannot be obtained. Therefore, this method cannot provide enough information for an effective resolution of resonance. In order to compensate for the lack of spectrum analysis, scholars have developed modal techniques that originate from structural dynamics. In [7], Prof. Xu proposed resonant modal analysis methods that were applied to the resonance analysis of power systems. In addition, the modal method was further

Manuscript received Apr. 20, 2017; accepted Dec. 30, 2017

Recommended for publication by Associate Editor Sung-Jin Choi.

[†]Corresponding Author: wujianhit@hotmail.com

Tel: +86-0451-86413420, Fax: +86-0451-86413420, Harbin Inst. Tech.

^{*}School of Electrical Eng. and Autom., Harbin Inst. of Tech., China

improved in [8]. However, this method can only determine the frequency and location of resonance.

In the suppression of resonance, the selection of the suppression method is related to the system components resulting in resonance. Sensitivity analysis is widely used in power systems. However, there are few studies on systems with multiple inverters connected to a grid. In [9], [10], the sensitivity theory was applied to parallel resonance analysis based on the nodal admittance matrix modal analysis method, and the equation of the element sensitivity is deduced to obtain the participation of system components in resonance. The resonant sensitivity of the system components is analyzed by using a real matrix, which simplifies the calculation process [11], [12]. When compared with the circuit simulation analysis based on frequency response, the sensitivity analysis obtains the resonant frequency of the system, and acquires the resonant loop, the resonant center point and the resonant sensitivity of the element. The sensitivity analysis can comprehensively obtain the resonance characteristic of large scale systems including those with a large number of inverters and it is very important in terms of grid system planning and stability analysis.

In this paper, in order to obtain the degree of participation of each component in resonance, an impedance model of a grid-connected inverters is established. Then, the resonant frequency is obtained by modal analysis. Further, a sensitivity analysis theory based on a partial derivative is used to analyze information on the participation and resonant center of the system at specific resonance frequencies. Finally, a four-node grid-connected test system with dual inverters is built in the laboratory to verify the correctness and validity of the proposed sensitivity analysis method.

II. MODEL OF A GRID-CONNECTED INVERTER

This paper focuses on the output characteristics of grid-connected inverters, regardless of the specific form of energy or the capacitor voltage fluctuations of the DC side. A typical voltage-source two-level three-phase inverter circuit structure is shown in Fig. 1.

In order to simplify the modeling, take the controller in the $\alpha\beta$ stationary coordinate system. The variable transformation is only after a Clark transformation, not through a Park transformation. In addition, there is no coupling between the α -axis and the β -axis, and the variables are independent. Similarly, after a Clark inverse transformation, the outputs of the three-phase model are independent of each other. In this way, the task of solving the three-phase grid-connected inverter output model is simplified into the task of solving a single-phase inverter output model.

The grid-connected inverter adopts a double-closed-loop control system, where the outer loop is the grid-connected current feedback and the inner loop is the capacitor current

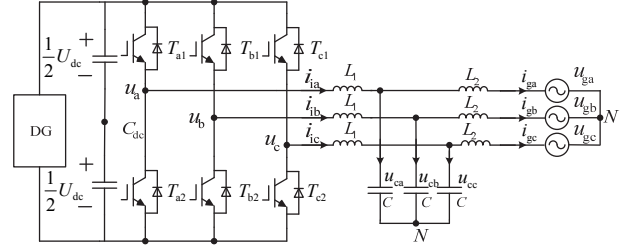


Fig. 1. Topology of a two-level voltage source inverter.

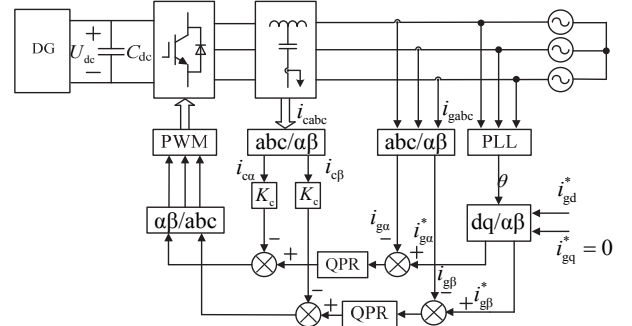


Fig. 2. Control strategy of a grid-connect inverter with proportional-resonant controllers.

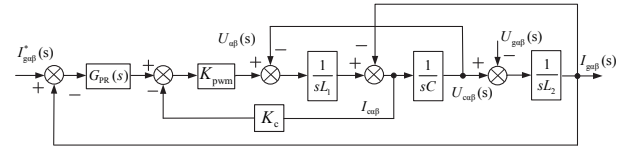


Fig. 3. Control block diagram of a system in the $\alpha\beta$ coordinate.

feedback. The controller takes quasi-proportional resonance control (QPR). Fig. 2 illustrates the control strategy structure.

The QPR controller transfer function is as follows:

$$G_{PR}(s) = k_p + \frac{k_r \omega_c s}{s^2 + 2\omega_c s + \omega_0^2} \quad (1)$$

According to the control strategy, the control block diagram of a three-phase grid-connected inverter with a LCL filter system is obtained under the $\alpha\beta$ coordinate, as shown in Fig. 3, where K_{pwm} is the gain of the inverter and K_c is the gain of the capacitor current feedback.

For further simplification, the system is expressed by a Norton equivalent circuit. Since an inverter is essentially a controlled current source, the current source and impedance parallel model of the inverter can be obtained in the $\alpha\beta$ static coordinate system, as shown in Fig. 4. $G(s)$ is the controlled current source coefficient and $Y(s)$ is the equivalent output admittance, in the complex frequency domain.

$$G(s) = \frac{K_{pwm} G_{PR}(s)}{L_1 L_2 C \cdot s^3 + K_{pwm} K_c L_2 C \cdot s^2 + (L_1 + L_2)s + K_{pwm} G_{PR}(s)} \quad (2)$$

$$Y(s) = \frac{L_1 C \cdot s^2 + K_{pwm} K_c C \cdot s + 1}{L_1 L_2 C \cdot s^3 + K_{pwm} K_c L_2 C \cdot s^2 + (L_1 + L_2)s + K_{pwm} G_{PR}(s)} \quad (3)$$

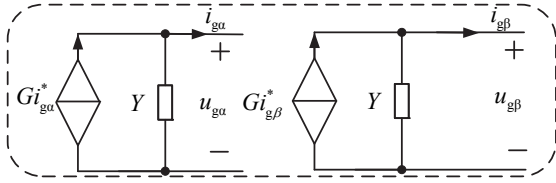


Fig. 4. Norton's equivalent circuits.

III. RESONANCE SENSITIVITY ANALYSIS THEORY

The purpose of resonant sensitivity analysis is to analyze the relationship between the parameter changes of a network component and the resonant characteristics of a system. According to the modal analysis theory, the resonance characteristic can be characterized by the eigenvalues of the network matrix [10], [11]. Therefore, the influence of the network component on the resonant characteristics can be quantitatively analyzed by partial derivatives of the eigenvalues of the network matrix to the network component parameters.

In order to facilitate the analysis, this paper takes the derivation process of the eigenvalue to component into the derivation process of the system matrix to component. Furthermore, the derivation process is taken into the product of derivation of the system matrix to element of the matrix and the derivation of the element of the matrix to component.

The resonant sensitivity analysis is based on the network matrix of the system, the node admittance matrix Y is established for the parallel resonances, and the circuit impedance matrix Z is established for the series resonances. Here, the network matrix D is expressed uniformly. The decomposition of the system network matrix is shown as:

$$\mathbf{D} = \mathbf{L}\mathbf{A}\mathbf{T} \quad (4)$$

where $\mathbf{L} = [l_1, \dots, l_k, \dots]^T$, $\mathbf{T} = [t_1, \dots, t_k, \dots]^T$, l_k is the k -th column element of \mathbf{L} , t_k is the k -th row element of the right eigenvector matrix \mathbf{T} , $\mathbf{A} = \text{diag}(\lambda_1, \dots, \lambda_k, \dots)$ is the diagonal characteristic matrix, and λ_k is the k -th eigenvalue of the eigenvalue matrix. Define the inverse eigenvalues of the network matrix Λ_k^{-1} to be Y_k , and the k -th modal is defined as:

$$Y_k = \frac{1}{\lambda_k} \quad (5)$$

First, the relationship between the left and right eigenmaps obtained by decomposition is derived as follows:

$$\begin{cases} \mathbf{T} = [t_1, \dots, t_k, \dots]^T \\ \mathbf{L} = [l_1, \dots, l_k, \dots]^T \\ \mathbf{L} = \mathbf{T}^{-1} \end{cases} \Rightarrow \mathbf{T}\mathbf{L} = \mathbf{I} \Rightarrow t_k l_k = 1 \quad (6)$$

For Eq. (4), both sides of the equation are left multiplied by the right eigenvector matrix $\mathbf{L}^T \mathbf{D} = \mathbf{L}^T \mathbf{L} \mathbf{A} \mathbf{T}$:

$$t_k \mathbf{D} = \lambda_k t_k \quad (7)$$

For Eq. (4), both sides of the equation are multiplied by the left eigenvector matrix $\mathbf{D}\mathbf{T}^{-1} = \mathbf{L}\mathbf{A}\mathbf{T}\mathbf{T}^{-1}$, which can be simplified as:

$$\mathbf{D}\mathbf{l}_k = \lambda_k \mathbf{l}_k \quad (8)$$

Assuming that α is the network component parameter, the partial derivative of Eq. (7) can be obtained with respect to α :

$$t_k \frac{\partial \mathbf{D}}{\partial \alpha} + \frac{\partial t_k}{\partial \alpha} \mathbf{D} = \frac{\partial \lambda_k}{\partial \alpha} t_k + \lambda_k \frac{\partial t_k}{\partial \alpha} \quad (9)$$

Both sides of Eq. (9) are multiplied by l_k :

$$\frac{\partial \lambda_k}{\partial \alpha} = t_k \frac{\partial \mathbf{D}}{\partial \alpha} l_k \quad (10)$$

It can be seen that the element sensitivity, which is the partial derivative of the eigenvalue to the element, can be obtained by solving the partial derivative of the network matrix D with respect to the system element. Therefore, the relationships among the network matrix D , the matrix elements and the system elements are analyzed.

Taking the partial derivative of the network matrix D with respect to the i th row, the j th column element \mathbf{D}_{ij} is shown as:

$$\frac{\partial \mathbf{D}}{\partial \mathbf{D}_{ij}} = \begin{pmatrix} \dots & \dots & 0 & \dots \\ 0 & 0 & 1 & 0 \\ \dots & \dots & 0 & \dots \\ \dots & \dots & 0 & \dots \end{pmatrix} i \quad (11)$$

From the above equation, it can be seen that only the elements in the i th row and the j th column are 1, and that the others elements are zero. From Eq. (10) and Eq. (11) the following can be obtained:

$$\frac{\partial \lambda_k}{\partial \mathbf{D}_{ij}} = t_k \frac{\partial \mathbf{D}}{\partial \mathbf{D}_{ij}} l_k = t_k \begin{pmatrix} \dots & \dots & 0 & \dots \\ 0 & 0 & 1 & 0 \\ \dots & \dots & 0 & \dots \\ \dots & \dots & 0 & \dots \end{pmatrix} l_k = l_{jk} t_{ki} \quad (12)$$

From Eq. (12), the partial derivative of the eigenvalue to the matrix in the network matrix D can be solved by the left and right eigenvector elements. Define the sensitivity matrix as Eq. (13), which is:

$$\mathbf{S}_\lambda = \mathbf{l}_k \mathbf{t}_k = \begin{pmatrix} \dots & * & \dots & \dots \\ \dots & * & \dots & \dots \\ * & t_{ki} l_{jk} & * & * \\ \dots & * & \dots & \dots \end{pmatrix} \quad (13)$$

Therefore, the sensitivity of the eigenvalue to the element \mathbf{D}_{ij} in the i th row and the j th column of the loop impedance matrix can be expressed by the elements of the sensitivity matrix as follows:

$$\frac{\partial \lambda_k}{\partial \mathbf{D}_{ij}} = S_{\lambda,ji} \quad (14)$$

A. Series Resonant Sensitivity

The series resonant sensitivity analysis is based on a loop impedance matrix. The elements of the matrix are made up of the elements for each of the circuits in the system. The first type of components only participates in the circuit i . These components are only involved in the composition of the diagonal elements. The second type of elements is involved in the formation of the diagonal elements Z_{ii} , which also constitutes to the non-diagonal elements Z_{ij} . These elements have an impact on the diagonal and off-diagonal elements of the impedance matrix.

1) The first type of network components only has an impact on the parameter Z_{ii} in the impedance matrix, and the network component parameters are denoted by $Z_{se} = R + jX$.

$$\frac{\partial \lambda_k}{\partial Z_s} = \mathbf{t}_k \frac{\partial Z}{\partial Z_{ii}} \frac{\partial Z_{ii}}{\partial Z_s} \mathbf{I}_k = l_{ik} t_{ki} = S_{\lambda,ii} \quad (15)$$

In order to simplify the problem, the elements can be divided into real and imaginary parts. Then the sensitivity of the eigenvalues for the real part and imaginary part of the first kind of network components can be obtained as:

$$\frac{\partial |\lambda_k|}{\partial R} = \frac{d|\lambda_k|}{dF} \frac{\partial F}{\partial R} = \frac{S_{r,ij} \lambda_r + S_{i,ij} \lambda_i}{\sqrt{\lambda_r^2 + \lambda_i^2}} \quad (16)$$

$$\frac{\partial |\lambda_k|}{\partial X} = \frac{d|\lambda_k|}{dF} \frac{\partial F}{\partial X} = \frac{S_{r,ij} \lambda_i - S_{i,ij} \lambda_r}{\sqrt{\lambda_r^2 + \lambda_i^2}} \quad (17)$$

where $\lambda_k = \lambda_r + j\lambda_i$, $S_{\lambda,ij} = S_r + jS_i$ and $F = |\lambda_k|^2$ is the intermediate variable set in the derivation process, and the sensitivity of the eigenvalue to the element is obtained by solving the derivative relation of F to the element.

2) For the second type of network components, assuming that the components are in parallel between loop i and loop j , there are:

$$\begin{aligned} \frac{\partial \lambda_k}{\partial Z_s} &= \mathbf{t}_k \left(\frac{\partial Z}{\partial Z_{ii}} \frac{\partial Z_{ii}}{\partial Z_s} + \frac{\partial Z}{\partial Z_{ij}} \frac{\partial Z_{ij}}{\partial Z_s} + \frac{\partial Z}{\partial Z_{ji}} \frac{\partial Z_{ji}}{\partial Z_s} + \frac{\partial Z}{\partial Z_{jj}} \frac{\partial Z_{jj}}{\partial Z_s} \right) \mathbf{I}_k \\ &= \mathbf{t}_k \left(\frac{\partial Z_{ii}}{\partial Z_s} + \frac{\partial Z_{ij}}{\partial Z_s} + \frac{\partial Z_{ji}}{\partial Z_s} + \frac{\partial Z_{jj}}{\partial Z_s} \right) \mathbf{I}_k = S_{\lambda,ii} - S_{\lambda,ji} - S_{\lambda,ij} + S_{\lambda,jj} \end{aligned} \quad (18)$$

Each part of Eq. (18) can be solved similar to the solving process for the sensitivity of the first kind of elements. In the resonance analysis, the form of $Y_s = G + jB$ is generally used for denoting the admittance. In this paper, the derivation of the admittance parameter is based on the derivation of the eigenvalue of the impedance parameter Z_s , and the sensitivity of the admittance parameters is obtained. Suppose $\partial \lambda_k / \partial R = \mu$, $\partial \lambda_k / \partial X = \nu$, which gives:

$$\frac{\partial R}{\partial G} = \frac{B^2 - G^2}{G^2 + B^2}, \quad \frac{\partial R}{\partial B} = \frac{-2GB}{G^2 + B^2} \quad (19)$$

$$\frac{\partial X}{\partial G} = \frac{2GB}{G^2 + B^2}, \quad \frac{\partial X}{\partial B} = \frac{G^2 - B^2}{G^2 + B^2} \quad (20)$$

For the admittance element, the sensitivity solution formula of the conductivity is:

$$\frac{\partial |\lambda_k|}{\partial G} = \frac{\partial |\lambda_k|}{\partial R} \frac{\partial R}{\partial G} + \frac{\partial |\lambda_k|}{\partial X} \frac{\partial X}{\partial G} = \frac{\mu (B^2 - G^2) + 2\nu GB}{(G^2 + B^2)^2} \quad (21)$$

For the admittance element, the sensitivity solution formula of the susceptance is:

$$\frac{\partial |\lambda_k|}{\partial B} = \frac{\partial |\lambda_k|}{\partial R} \frac{\partial R}{\partial B} + \frac{\partial |\lambda_k|}{\partial X} \frac{\partial X}{\partial B} = \frac{\nu (B^2 - G^2) - 2\mu GB}{(G^2 + B^2)^2} \quad (22)$$

B. Parallel Resonant Sensitivity

The parallel resonance sensitivity analysis is based on the node admittance matrix Y_p . The elements of the matrix are made up of the elements of each node in the system. The first type of element is the element associated with node i , which only participates in the formation of the diagonal elements. The second type of element is an element connected in series between node i and node j , which participates in forming both the diagonal element Y_{ii} and the non-diagonal element Y_{ij} .

1) For the first type of network components, assuming that the components are connected in node i , which only effects the parameter Y_{ii} in the admittance matrix, the network component parameters are denoted by $Y_p = G + jB$.

$$\frac{\partial \lambda_k}{\partial Y_p} = \mathbf{t}_k \frac{\partial Y}{\partial Y_{ii}} \frac{\partial Y_{ii}}{\partial Y_p} \mathbf{I}_k = l_{ik} t_{ki} = S_{\lambda,ii} \quad (23)$$

The sensitivity of the eigenvalues for the conductivity and acceptance of the first kind of network components can be obtained as:

$$\frac{\partial |\lambda_k|}{\partial G} = \frac{d|\lambda_k|}{dF} \frac{\partial F}{\partial G} = \frac{S_{r,ij} \lambda_r + S_{i,ij} \lambda_i}{\sqrt{\lambda_r^2 + \lambda_i^2}} \quad (24)$$

$$\frac{\partial |\lambda_k|}{\partial B} = \frac{d|\lambda_k|}{dF} \frac{\partial F}{\partial B} = \frac{S_{r,ij} \lambda_i - S_{i,ij} \lambda_r}{\sqrt{\lambda_r^2 + \lambda_i^2}} \quad (25)$$

where $\lambda_k = \lambda_r + j\lambda_i$, $S_{\lambda,ij} = S_r + jS_i$ and $F = |\lambda_k|^2$ is the intermediate variable set in the derivation process.

2) For the second type of network components, assuming that the components are in series between node i and node j , that is:

$$\begin{aligned} \frac{\partial \lambda_k}{\partial Y_p} &= \mathbf{t}_k \left(\frac{\partial Y}{\partial Y_{ii}} \frac{\partial Y_{ii}}{\partial Y_p} + \frac{\partial Y}{\partial Y_{ij}} \frac{\partial Y_{ij}}{\partial Y_p} + \frac{\partial Y}{\partial Y_{ji}} \frac{\partial Y_{ji}}{\partial Y_p} + \frac{\partial Y}{\partial Y_{jj}} \frac{\partial Y_{jj}}{\partial Y_p} \right) \mathbf{I}_k \\ &= \mathbf{t}_k \left(\frac{\partial Y_{ii}}{\partial Y_p} + \frac{\partial Y_{ij}}{\partial Y_p} + \frac{\partial Y_{ji}}{\partial Y_p} + \frac{\partial Y_{jj}}{\partial Y_p} \right) \mathbf{I}_k = S_{\lambda,ii} - S_{\lambda,ji} - S_{\lambda,ij} + S_{\lambda,jj} \end{aligned} \quad (26)$$

Each part of Eq. (26) can be solved according to the solving process of the sensitivity of the first kind of elements. As in the parallel resonance analysis, the impedance form of $Z_p = R + jX$ is generally used. In this paper, the derivation of

the impedance parameter is based on the derivation of the eigenvalue of the admittance parameter Y_p . The sensitivity of the impedance parameters can be obtained by supposing $\partial\lambda_k/\partial G = \mu$, $\partial\lambda_k/\partial B = \nu$, which yields:

$$\frac{\partial G}{\partial R} = \frac{X^2 - R^2}{R^2 + X^2}, \quad \frac{\partial G}{\partial X} = \frac{-2RX}{R^2 + X^2} \quad (27)$$

$$\frac{\partial B}{\partial R} = \frac{2RX}{R^2 + X^2}, \quad \frac{\partial B}{\partial X} = \frac{R^2 - X^2}{R^2 + X^2} \quad (28)$$

The sensitivity solution formula of the impedance component resistance part is expressed as follows:

$$\frac{\partial|\lambda_k|}{\partial R} = \frac{\partial|\lambda_k|}{\partial G} \frac{\partial G}{\partial R} + \frac{\partial|\lambda_k|}{\partial B} \frac{\partial B}{\partial R} = \frac{\mu(X^2 - R^2) + 2\nu RX}{(R^2 + X^2)^2} \quad (29)$$

The sensitivity solution formula of the impedance component reactance part is expressed as follows:

$$\frac{\partial|\lambda_k|}{\partial X} = \frac{\partial|\lambda_k|}{\partial G} \frac{\partial G}{\partial X} + \frac{\partial|\lambda_k|}{\partial B} \frac{\partial B}{\partial X} = \frac{\nu(X^2 - R^2) - 2\mu RX}{(R^2 + X^2)^2} \quad (30)$$

C. Normalized Resonance Sensitivity

In the last section, both the real part and the imaginary part sensitivity value for each system component are obtained. This reflects the sensitivity of the matrix eigenvalues for the changes of the component parameters. It does not take the relationship between the components into account. There is no reference value. Making a unified standard for the sensitivity value, which is expressed as a percentage, the normalized sensitivity solution formula is shown as:

$$\frac{\partial|\lambda_k|}{\partial\alpha} = \frac{\partial|\lambda_k|/\lambda_k}{\partial\alpha/\alpha} = \frac{\partial\lambda_k}{\partial\alpha} * \frac{\alpha}{\lambda_k} \quad (31)$$

where $\partial\lambda_k/\lambda_k$ and $\partial\alpha/\alpha$ represent the relative change of the eigenvalue and the parameter, respectively. The sensitivity analysis of the normalized sensitivity becomes more practical [13].

IV. RESONANCE ANALYSIS OF AN ACTIVE DISTRIBUTION NETWORK

A. Analysis of Series Resonant Sensitivity

A four-node grid-connected test system with dual inverters has been built. Fig. 5 shows an impedance model of the four-node grid-connected test system. Z_g is the grid impedance, Y_{N1} is the equivalent admittance of inverter 1, Y_{N2} is the equivalent admittance of inverter 1, Y_{LC1} is the equivalent admittance of load branch 1, and Y_{LC2} is the equivalent admittance of load branch 2. Z_{L1} , Z_{L2} and Z_{L3} are the line impedances.

The series sensitivity analysis was performed by Eq. (16), Eq. (17), Eq. (21) and Eq. (22). As an example of the components Z_g and Y_{LC1} , a detailed formula for solving the sensitivity is given.

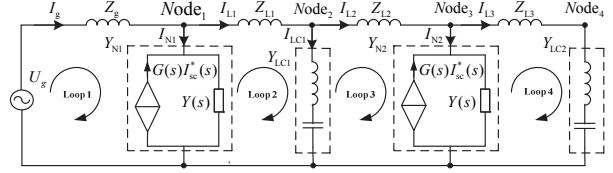


Fig. 5. Impedance model of a four-node grid-connected system.

First, the circuit impedance matrix Z is given.

$$Z = \begin{bmatrix} Z_g + 1/Y_{N1} & -1/Y_{N1} & 0 & 0 \\ -1/Y_{N1} & 1/Y_{N1} + Z_{L1} + 1/Y_{LC1} & -1/Y_{LC1} & 0 \\ 0 & -1/Y_{LC1} & 1/Y_{LC1} + Z_{L2} + 1/Y_{N2} & -1/Y_{N2} \\ 0 & 0 & -1/Y_{N2} & 1/Y_{N2} + Z_{L3} + 1/Y_{LC2} \end{bmatrix} \quad (32)$$

From the circuit impedance matrix formula it can see that only the element Z_{11} contains the element Z_g . This means that the component is only involved in loop 1, and it participates in the loop impedance matrix construction in impedance form. It can be learned that both the real part and the imaginary part of the sensitivity solution formula are as follows:

$$\frac{\partial|\lambda_k|}{\partial R_{Z_g}} = \frac{S_{r,11}\lambda_r + S_{i,11}\lambda_i}{\sqrt{\lambda_r^2 + \lambda_i^2}} \quad (33)$$

$$\frac{\partial|\lambda_k|}{\partial X_{Z_g}} = \frac{S_{r,11}\lambda_r + S_{i,11}\lambda_i}{\sqrt{\lambda_r^2 + \lambda_i^2}} \quad (34)$$

For Y_{LC1} , since it forms the elements Z_{22} , Z_{33} , Z_{23} and Z_{32} of the loop impedance matrix, and participates in the loop impedance matrix construction in the admittance form, it can be seen that the imaginary part sensitivity formula of Y_{LC1} consists of the four parts as follows:

$$\frac{\partial|\lambda_k|}{\partial G_{Y_{LC1}}} = \frac{\nu(B_{Y_{LC1}}^2 - G_{Y_{LC1}}^2) + 2\mu G_{Y_{LC1}} B_{Y_{LC1}}}{(G_{Y_{LC1}}^2 + B_{Y_{LC1}}^2)^2} \quad (35)$$

$$\frac{\partial|\lambda_k|}{\partial B_{Y_{LC1}}} = \frac{\nu(B_{Y_{LC1}}^2 - G_{Y_{LC1}}^2) - 2\mu G_{Y_{LC1}} B_{Y_{LC1}}}{(G_{Y_{LC1}}^2 + B_{Y_{LC1}}^2)^2} \quad (36)$$

where $\nu = \nu_{22} + \nu_{33} - \nu_{23} - \nu_{32}$ and $\mu = \mu_{22} + \mu_{33} - \mu_{23} - \mu_{32}$.

In the same way, the resonant sensitivity formula of the other circuit impedances can be obtained. The system components are divided into two parts, the real part and the imaginary part. There are 16 cases, and the normalized sensitivity can be obtained.

The inverter parameters are presented in Table I, and the four-node test system parameter design is presented in Table II, where Y is the equivalent output admittance, as shown in Eq. (3). Then based on the modal analysis, the frequency and the location of the series resonance can be obtained, as shown in Fig. 6.

It can be seen that there are four resonant peaks in the system. Based on the series resonant sensitivity analysis method, the resonant sensitivity of the system is analyzed at

TABLE I
 PARAMETERS OF A GRID-CONNECTED CONVERTER

Name of Unit	Value	Name of Unit	Value
L_1	1.3mH	K_p	10
L_2	0.2 mH	K_c	10
C	20 μ F	K_r	200
U_{dc}	800V	ω_c	5rad/s
U_g	380V	f_s	10kHz
I_N	14A	S_N	10KW

 TABLE II
 PARAMETER OF THE FOUR-NODE GRID-CONNECTED TEST SYSTEM

Name of Unit	Value	Name of Unit	Value
Z_g	0.01 Ω ,0.32mH	Y_{N1}	Y
Z_{L1}	0.05 Ω ,0.128mH	Y_{LC1}	47 μ F
Z_{L2}	0.064mH	Y_{N2}	Y
Z_{L3}	0.04 Ω ,4mH	Y_{LC2}	0.04 Ω ,41.3uF

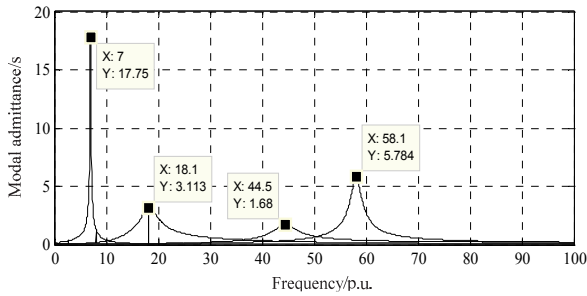


Fig. 6. Modal analysis results of the series harmonic resonance.

four resonant frequencies, the sensitivity matrix and the eigenvalues are obtained, and the sensitivity of the element is obtained, which is expressed by the normalized sensitivity. It is worth noting that, although the imaginary part and the real part of the system components are solved separately, there are 16 sensitivity values. However, since the main components participating in the resonance are the imaginary part, the sensitivity of the eight imaginary part in the four-node system is extracted, as shown in Fig. 7 to Fig. 10.

For the 7th harmonic series resonant sensitivity, whose frequency is 350Hz, Fig. 7 shows that the component which has larger influence is the imaginary part of the line impedance Z_{L3} and the grid impedance Z_g , followed by the load Y_{LC1} . Meanwhile the influence of other components are relatively small.

For the 17th harmonic series resonant sensitivity, whose frequency is 850Hz, Fig. 8 shows that the components with the largest influence are the capacitive load Y_{LC1} , the inverter Y_{N1} and the inverter Y_{N2} . The next are the grid impedance Z_g , the line impedance Z_{L1} and the line impedance Z_{L3} , while the other components show less impact.

For the 43th series harmonic resonance sensitivity, whose frequency is 2150Hz, Fig. 9 shows that the components with the largest influence are the imaginary part of the inverter Y_{N1} ,

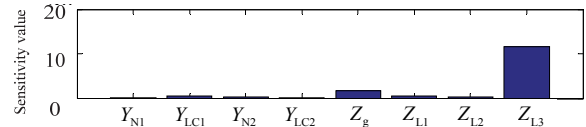


Fig. 7. Sensitivity of the series resonance on the 7th order harmonic.

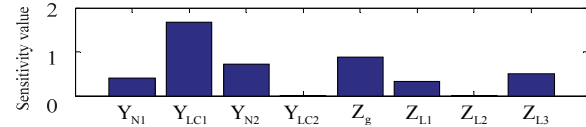


Fig. 8. Sensitivity of the series resonance on the 17th order harmonic.

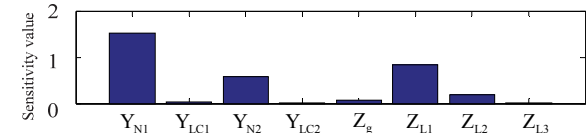


Fig. 9. Sensitivity of the series resonance on the 43th order harmonic.

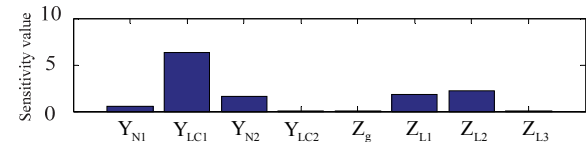


Fig. 10. Sensitivity of the series resonance on the 57th order harmonic.

inverter Y_{N2} and load Y_{LC2} , followed by the line impedances Z_{L1} and Z_{L2} , while other components are less significant.

For the 57th harmonic series resonant sensitivity, whose frequency is 2850Hz, Fig. 10 shows that that the component with the largest influence is the capacitive load Y_{LC1} . The next is the imaginary part of the inverter Y_{N1} , the line impedance Z_{L1} and the line impedance Z_{L2} , while other components are less significant.

B. Analysis of Parallel Resonant Sensitivity

The four-node system shown in Fig.5 is used for a parallel sensitivity analysis. First, the system node admittance matrix Y is given by:

$$Y = \begin{bmatrix} \frac{1}{Z_g} + Y_{N1} + \frac{1}{Z_{L1}} & -\frac{1}{Z_{L1}} & 0 & 0 \\ -\frac{1}{Z_{L1}} & \frac{1}{Z_{L1}} + Y_{LC1} + \frac{1}{Z_{L2}} & -\frac{1}{Z_{L2}} & 0 \\ 0 & -\frac{1}{Z_{L2}} & \frac{1}{Z_{L2}} + Y_{N2} + \frac{1}{Z_{L3}} & -\frac{1}{Z_{L3}} \\ 0 & 0 & -\frac{1}{Z_{L3}} & -\frac{1}{Z_{L3}} + Y_{LC2} \end{bmatrix} \quad (37)$$

Here an example of solving the sensitivities of Z_{L1} and Y_{N1} are given. From the node admittance matrix formula it can be seen that only the element Y_{11} contains the element Y_{N1} . In other words, the component is only involved in node 1, and it participates in the node admittance matrix construction in admittance form. It can be learned that the real part and

imaginary part of the sensitivity solution formula are as follows:

$$\frac{\partial |\lambda_k|}{\partial G_{Y_{N1}}} = \frac{S_{r,11} \lambda_r + S_{i,11} \lambda_i}{\sqrt{\lambda_r^2 + \lambda_i^2}} \quad (38)$$

$$\frac{\partial |\lambda_k|}{\partial B_{Y_{N1}}} = \frac{S_{r,11} \lambda_r + S_{i,11} \lambda_i}{\sqrt{\lambda_r^2 + \lambda_i^2}} \quad (39)$$

For the element Z_{L1} , since it forms the elements Y_{11} , Y_{22} , Y_{12} and Y_{21} of the node admittance matrix, and it participates in the node admittance matrix construction in the impedance form, it can be seen that the real part and imaginary part sensitivity formulas are as follows:

$$\frac{\partial |\lambda_k|}{\partial R_{Z_1}} = \frac{\mu (X_{Z_1}^2 - R_{Z_1}^2) + 2\nu R_{Z_1} X_{Z_1}}{(R_{Z_1}^2 + X_{Z_1}^2)^2} \quad (40)$$

$$\frac{\partial |\lambda_k|}{\partial X_{Z_1}} = \frac{\nu (R_{Z_1}^2 - X_{Z_1}^2) - 2\mu R_{Z_1} X_{Z_1}}{(R_{Z_1}^2 + X_{Z_1}^2)^2} \quad (41)$$

where $\mu = \mu_{11} + \mu_{22} - \mu_{12} - \mu_{21}$ and $\nu = \nu_{11} + \nu_{22} - \nu_{12} - \nu_{21}$.

In the same way, the resonant sensitivity formulas of the other circuit impedances can be obtained. The system components are divided into two parts, the real part and the imaginary part. There are 16 cases, and the normalized sensitivity can be obtained. The analysis results are shown in Fig. 11. It can be seen that there are four resonant peaks in the system. Based on the parallel resonant sensitivity analysis theory, the resonant sensitivity of the system is analyzed at four resonant frequencies.

Similar to the series sensitivity analysis, only the sensitivity values of the imaginary parts of the system elements are given, as shown in Fig. 12 to Fig. 15.

For the 7th harmonic parallel resonant sensitivity, which has a frequency of 350Hz, Fig. 12 shows that the components having largest influence are the imaginary part of the line impedance Z_{L3} and the load Y_{LC2} , followed by the imaginary part of the line impedance Z_{L1} and the line impedance Z_{L2} , while the impacts of the other components are relatively minor.

For the 17th harmonic parallel resonant sensitivity, which has a frequency of 850Hz, Fig. 13 shows that the components with the largest influence are the imaginary part of the grid impedance Z_g and the load Y_{LC1} , followed by the imaginary part of the inverter Y_{N2} , inverter Y_{N1} , the line impedance Z_{L1} and the line impedance Z_{L3} , while the impacts of the other components are relatively minor.

For the 43th harmonic parallel resonant sensitivity, which has a frequency of 2150Hz, Fig. 14 shows that the components with the largest influence are the imaginary part of the inverter Y_{N2} , the line impedance Z_{L1} and the line impedance Z_{L2} , followed by the imaginary part of the inverter Y_{N1} , while the impacts of the other components are relatively minor.

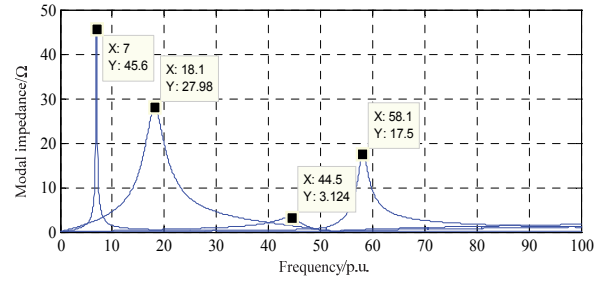


Fig. 11. Modal analysis results of the parallel harmonic resonance.

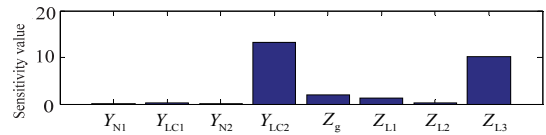


Fig. 12. Sensitivity of the parallel resonance on the 7th order harmonic.

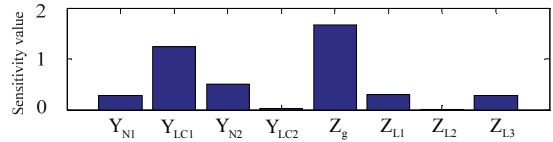


Fig. 13. Sensitivity of the parallel resonance on the 17th order harmonic.

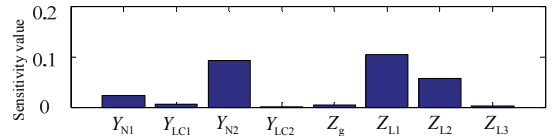


Fig. 14. Sensitivity of the parallel resonance on the 43th order harmonic.

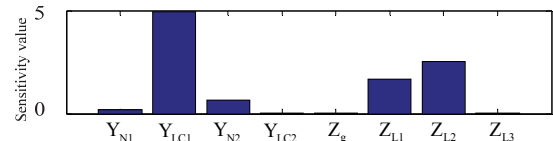


Fig. 15. Sensitivity of the parallel resonance on 5 the 7th order harmonic.

For the 57th harmonic parallel resonant sensitivity, which has a frequency of 2850Hz, Fig. 15 shows that the components with the largest influence are the imaginary part of load Y_{LC1} , the line impedance Z_{L1} and the line impedance Z_{L2} , followed by the inverter Y_{N2} , while the impacts of the other components are relatively minor.

V. EXPERIMENTAL RESULTS ANALYSIS

The proposed resonance analysis method based on sensitivity is verified by experiments carried out on a four-node grid-connected laboratory prototype, where the circuit

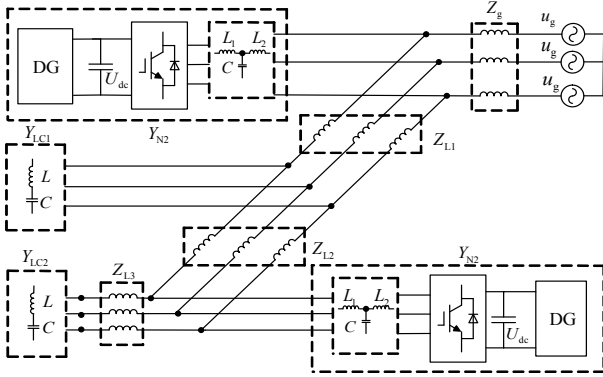


Fig. 16. Configuration of the experimental system.

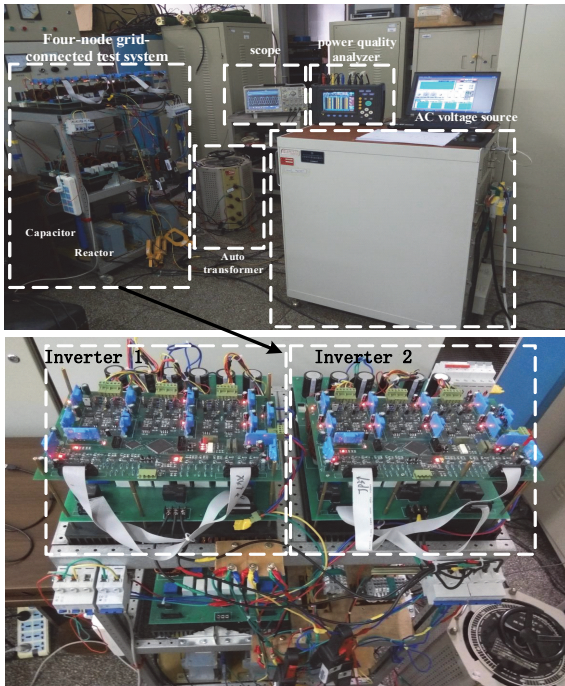


Fig. 17. Setup of the experimental system.

structure is the same as that shown in Fig. 5. The setup of the experimental system is shown in Fig. 16 and Fig. 17. The experimental grid-connected system consists of two three-phase inverters supplied by a standard three-phase rectifier, a three line impedance and a two load impedance. For the inverter, no DC voltage loop is used. The digital controllers consist of a DSP (TMS320F28335) and a CPLD. The parameters of the grid-connected inverter are listed in Table I and the four-node system parameters are listed in Table II. A programmable voltage source is used to inject voltage harmonics to the series loop and an active power filter (APF) is used to inject current harmonics to the node of the experiment system.

A. Analysis of Series Resonance

For the four-node test system, based on the series sensitivity analysis in the previous section, the 7th harmonic is

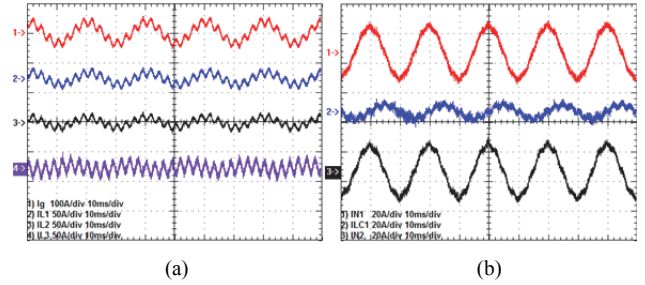

 Fig. 18. Waveforms of the branch current with a 7th order harmonic voltage at the 4th-loop ($Z_{L3}=0.04 \Omega$, 4mH).

TABLE III
SENSITIVITY ANALYSIS VALUES OF THE SERIES RESONANCE ON THE 7TH ORDER HARMONIC

System element	Sensitivity value	System	Sensitivity value
Z_g	1.74	Y_{N1}	0.086
Z_{L1}	0.59	Y_{LC1}	0.43
Z_{L2}	0.24	Y_{N2}	0.21
Z_{L3}	11.6	Y_{LC2}	0.002

chosen for experimental verification. When loop four is injected with 3% 7th steady-state voltage harmonics emulated by a programmable voltage source, experiment waveforms of each branch current and the content of the 7th harmonic of each branch based on a FFT are detected. The sensitivity analysis results are validated by comparing the 7th harmonic distortion of each branch current with the normalized sensitivity of the components.

The waveforms for each of the branch currents I_g , I_{L1} , I_{L2} , I_{L3} , I_{N1} , I_{LC1} and I_{N2} are shown in Fig. 18. The sensitivity values of the system components in the 7th harmonic resonance are shown in Table III. The Contents of the 7th harmonic for each of the branches are shown in Table IV based on Fig. 18.

By comparing Table III with Table IV, it can be seen that the sensitivity of the imaginary part of the component Z_{L3} is the largest and that the current in the Z_{L3} branch has resonance at the 7th harmonic frequency and further causes the other branches to have the 7th harmonic current. The waveforms of the branch current with the 7th order harmonic voltage at the other loop are similar to those shown in Fig. 18, and the current in Z_{L3} branch also contains resonance at the 7th harmonic frequency. Thus, the key component of the resonance is Z_{L3} , which has a higher sensitivity value in the 7th resonant frequency. Therefore, the harmonic resonance can be eliminated by changing the parameters of Z_{L3} . In Fig. 19, when Z_{L3} is changed as 0.4mH, its sensitivity is reduced. At this time, the waveforms for each of the branch currents I_g , I_{L1} , I_{L2} , I_{L3} , I_{N1} , I_{LC1} and I_{N2} are shown in Fig. 20. None of the waveforms have been distorted. Therefore, the correctness of the sensitivity analysis is also explained.

TABLE IV
7TH HARMONIC CONTENTS OF THE BRANCH CURRENTS WITH SERIES RESONANCE

Current	Content of 7 th harmonic(A)	Current	Content of 7 th harmonic(A)
I_g	12.2	I_{N1}	2.0
I_{L1}	11.8	I_{LC1}	3.0
I_{L2}	10.7	I_{N2}	2.3
I_{L3}	10.4		

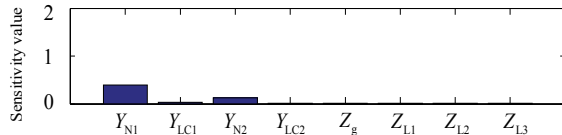


Fig. 19. Sensitivity of the series resonance on the 7th order harmonic ($Z_{L3}=0.04 \Omega$, 0.4mH).

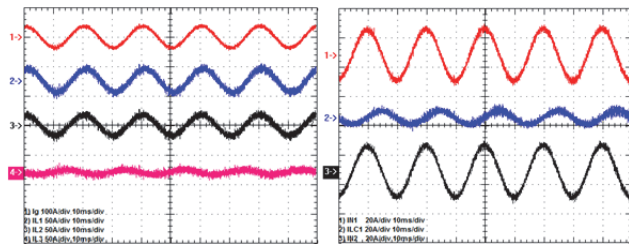


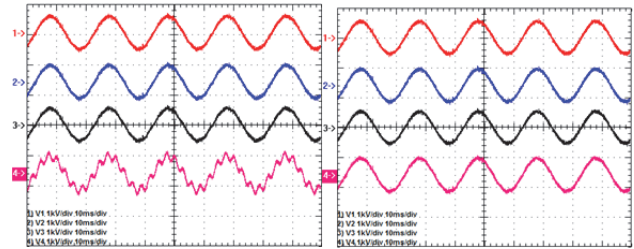
Fig. 20. Waveforms of the branch current with the 7th order harmonic voltage at the 4th-loop ($Z_{L3}=0.04 \Omega$, 0.4mH).

B. Analysis of Parallel Resonance

For the four-node test system, based on the parallel sensitivity analysis in the previous section, a 2A 7th harmonic current is injected into node 3 and node 4 for experimental verification. The node voltage is detected, as shown in Fig. 21. In addition, the 7th harmonic voltage content of Fig. 21 (a) is analyzed through a FFT. When node 4 is injected by harmonic current, the voltage of node 4 is distorted and the voltages of the other nodes are not distorted, as shown in Fig. 21 (a). When node 3 is injected with harmonic current, the voltage for all of the nodes is not distorted, as shown in Fig. 21 (b). When node 1 and node 2 are injected with harmonic current, the voltages are without distortions.

The sensitivity values of the system components in the 7th harmonic resonance shown in Table V and the 7th harmonic voltage content of Fig. 21 (a) are shown in Table VI.

When compared with Table V and Table VI, for the 7th resonance, the largest sensitivity value of the imaginary part of the system element is the load Y_{LC2} and the line impedance Z_{L3} , followed by the grid impedance Z_g and the line impedance Z_{L1} . The harmonic distortion of the experimental system also shows that the 7th harmonic voltage content of V_4 is the largest. In Fig. 22, when Z_{L3} is changed as 0.4mH, its sensitivity is reduced. At this time, the waveforms for each of the node voltages are shown in Fig. 23. None of the



(a) node 4 (b) node 3
Fig. 21. Waveforms of the node voltage with the 7th order harmonic current ($Z_{L3}=0.04 \Omega$, 4mH).

TABLE V
BASE UNITS SENSITIVITY ANALYSIS VALUE OF THE PARALLEL RESONANCE ON THE 7TH ORDER HARMONIC

System element	Sensitivity value	System element	Sensitivity value
Z_g	2.43	Z_{L2}	0.64
Y_{N1}	0.52	Y_{N2}	0.6
Z_{L1}	1.56	Z_{L3}	11.3
Y_{LC1}	0.58	Y_{LC2}	13.5

TABLE VI
7TH HARMONIC CONTENT OF THE NODE VOLTAGE WITH PARALLEL RESONANCE

Voltage	Content of 7 th harmonic (V)	Voltage	Content of 7 th harmonic (V)
V_1	6.8	V_3	10.2
V_2	9.5	V_4	81.3

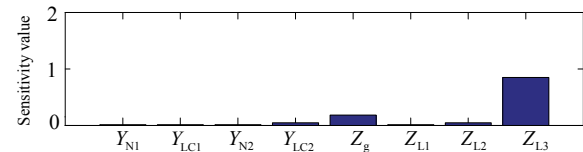


Fig. 22. Sensitivity of the parallel resonance on the 7th order harmonic ($Z_{L3}=0.04 \Omega$, 0.4mH).

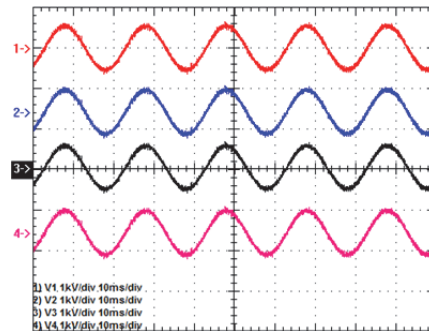


Fig. 23. Waveforms of the node voltage with the 7th order harmonic current at node 4 ($Z_{L3}=0.04 \Omega$, 0.4mH).

waveforms have been distorted. Therefore, the experimental results verify the correctness of the sensitivity analysis and confirm that the resonant center of the system is in node 4.

By observing the sensitivity analysis and the experimental results, it can be found that for the 7th harmonic resonance, the perceptual components with the larger influence is Z_{L3} , both in the series resonance and parallel resonances. However, for the capacitive components, the larger influence components are Y_{LC1} and Y_{N2} in the series resonance and Y_{LC2} in the parallel resonances. Note that there are 7th harmonic resonances in both the series resonances and the parallel resonances. However, the resonant elements are not identical. This also explains the necessity of separately analyzing the series resonances and the parallel resonances.

Resonance analysis results provide a reliable basis for harmonic suppression. According to the analysis results of the four nodes grid-connection test system, the most effective method of 7th resonance suppression is the parameter adjustment for Z_{L3} or adding a damping device in the resonant center of node 4, which is a further research direction.

VI. CONCLUSIONS

For a designated resonant frequency, this paper gives formulas of the series resonant normalized sensitivity of the network components. The formulas are adapted for the resonance sensitivity analysis of a four-node grid-connected test system, and the resonance sensitivity of each network component is obtained. The analysis results show that the sensitivities for the network component and resonant center of the system can be determined by the formulas. Moreover, the sensitivities and resonant center are different under different resonance frequencies. Experimental results verify the sensitivity analysis results of a grid-connected system.

ACKNOWLEDGMENT

This paper and its related research are supported by grants from the National Natural Science Foundation of China (51407043) and the National High Technology Research and Development Program 863 of China (2015AA050603).

REFERENCES

- [1] D. Xu, F. Wang, Y. Ruan, and H. Mao, "Output impedance modeling of grid-connected inverters considering nonlinear effects," in *2012 IEEE 13th Workshop on Control and Modeling for Power Electronics (COMPEL)*, pp. 1-7, 2012.
- [2] M. Lu, F. Blaabjerg, and X. Wang, "Interaction admittance based modeling of multi-paralleled grid-connected inverter with LCL-filter," in *2016 IEEE 2nd Annual Southern Power Electronics Conference (SPEC)*, pp. 1-7, 2016.
- [3] F. Wang, X. Feng, and C. Wu, "Research on grid harmonic interaction of multiple flyback micro-inverters," *Proceedings of the CSEE*, Vol. 36, No.3, pp. 709-716, May 2016.
- [4] X. Xiong, W. Zheng, K. Chen, J. Shen, "Identification approach in modeling a photovoltaic grid-tie inverter," *International Rev. Electrical Eng.*, Vol. 7, No. 3, pp. 4575-4584, 2012.
- [5] B. C. Smith, J. Arrillaga, A. R. Wood, and N. R. Watson, "A review of iterative harmonic analysis for AC-DC power systems," *IEEE Trans. Power Del.*, Vol. 13, No. 1, pp. 180-185, Jan. 1998.
- [6] A. Borner and T. Grebe, "Modelling and simulation of the propagation of harmonics in electric power networks. I." *IEEE Trans. Power Del.*, Vol. 11, No. 1, pp. 452-465, Jan. 1996.
- [7] W. Xu, Z. Huang, Y. Cui, and H. Wang, "Harmonic resonance mode analysis," *IEEE Trans. Power Del.*, Vol. 20, No. 2, pp.1182-1190, Apr. 2005.
- [8] C. Yang, K. Liu, and Q. Zhang, "An improved modal analysis method for harmonic resonance analysis," in *IEEE International Conference on Industrial Technology*, pp. 1-5, 2008.
- [9] Z. Huang, Y. Cui, and W. Xu, "Application of modal sensitivity for power system harmonic resonance analysis," *IEEE Trans. Power Syst.*, Vol. 22, No. 1, pp. 222-231, Feb. 2007.
- [10] Y. Cui and W. Xu, "Harmonic resonance mode analysis using real symmetrical nodal matrices," *IEEE Trans. Power Del.*, Vol. 22, No. 3, pp. 1989-1990, Jul. 2007.
- [11] Y. Cui and X. Wang, "Modal frequency sensitivity for power system harmonic resonance analysis," *IEEE Trans. Power Del.*, Vol. 27, No. 2, pp. 1010-1017, Apr. 2012.
- [12] H. Hu, Z. He, Y. Zhang, and S. Gao, "Modal frequency sensitivity analysis and application using complex nodal matrix," *IEEE Trans. Power Del.*, Vol. 29, No. 2, pp. 969-971, Apr. 2014.
- [13] Z. Huang, Y. Cui, and W. Xu, "Application of modal sensitivity for power system harmonic resonance analysis," *IEEE Trans. Power Syst.*, Vol. 22, No. 1, pp. 222-231, Feb. 2007.



Jian Wu was born in Harbin, China, in 1979. He received his B.S., M.S. and Ph.D. degrees in Electrical Engineering from the Harbin Institute of Technology (HIT), Harbin, China, in 2001, 2003 and 2007, respectively. He became a Lecturer in the Department of Electrical Engineering, HIT, in 2007. His current research interests include power quality, voltage source converter high-voltage direct current, the monitoring schemes for distribution networks, and multi-level converters.



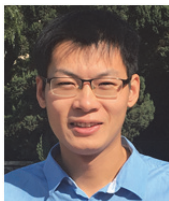
Wanqin Han was born in Chongqing, China, in 1994. She received her B.S. degree from the Harbin Institute of Technology (HIT), Harbin, China, in 2017, where she is presently working towards her M.S. degree in the School of Electrical Engineering and Automation. Her current research interests include high-power electronics, multilevel converters, and DC/DC converters.



Tao Chen was born in Chongqing, China, in 1994. He received his B.S. degree from the Harbin Institute of Technology (HIT), Harbin, China, in 2017, where he is presently working towards his M.S. degree in the School of Electrical Engineering and Automation. His current research interests include high-power electronics, multilevel converters, and DC/DC converters.



Jiaqi Zhao was born in Chongqing, China, in 1994. He received his B.S. degree from the Harbin Institute of Technology (HIT), Harbin, China, in 2016, where he is presently working towards his M.S. degree in the School of Electrical Engineering and Automation. His current research interests include high-power electronics, multilevel converters, and DC/DC converters.



Binbin Li obtained his B.S., M.S. and Ph.D. degrees in Electrical Engineering from the Harbin Institute of Technology (HIT), Harbin, China, in 2010, 2012 and 2017, respectively. From November 2015 to November 2016, he was a Visiting Researcher in the Department of Electronic and Electrical Engineering, University of Strathclyde, Glasgow, SCT, UK. He is presently working as an Associate Professor in the Department of Electrical Engineering, HIT. His current research interests include multilevel converters, high-power electronics, control algorithms, and pulse-width modulation techniques.



Dianguo Xu obtained his B.S. degree in Control Engineering from Harbin Engineering University, Harbin, China, in 1982; and his M.S. and Ph.D. degrees in Electrical Engineering from the Harbin Institute of Technology (HIT), Harbin, China, in 1984 and 1989, respectively. He became an Assistant Professor in the Department of Electrical Engineering, HIT, in 1984. He has been a Professor in the Department of Electrical Engineering, HIT, since 1994. He was the Dean of the School of Electrical Engineering and Automation, HIT, from 2000 to 2010. He is presently serving as the Vice President of HIT. His current research interests include renewable energy generation technology, multiterminal HVDC systems based on VSCs, power quality mitigation, speed sensorless vector-controlled motor drives, and high-performance PMSM servo systems. He has published over 600 technical papers in journals and conference proceedings. Professor Xu is an Associate Editor of the IEEE Transactions on Industrial Electronics and the IEEE Journal of Emerging and Selected Topics in Power Electronics. He is also serving as the Chairman of the IEEE Harbin Section, as the Director of the Lighting Power Supply Committee of the CPSS, and as the Vice Director of the Electric Automation Committee of the CAA, the Electrical Control System and Equipment Committee of the CES, and the Power Electronics Committee of the CES.